Nucl Eng Technol 47 (2015) 546–558

Available online at www.sciencedirect.com

ScienceDirect

journal homepage: http://www.journals.elsevier.com/nuclear-engineering-and-technology/

Original Article

A PROPOSAL ON ALTERNATIVE SAMPLING-BASED MODELING METHOD OF SPHERICAL PARTICLES IN STOCHASTIC MEDIA FOR MONTE CARLO SIMULATION

SONG HYUN KIM [a], JAE YONG LEE [a], DO HYUN KIM [a], JONG KYUNG KIM [a,*], and JAE MAN NOH [b]

[a] Department of Nuclear Engineering, Hanyang University, 222 Wangsimni-ro, Seoul 133-791, South Korea
[b] Korea Atomic Energy Research Institute, 111 Daedeok-daero, Daejeon 305-353, South Korea

ARTICLE INFO

Article history:
Received 2 October 2014
Received in revised form
24 February 2015
Accepted 1 March 2015
Available online 21 May 2015

Keywords:
Boundary effect
Chord length sampling
Monte Carlo
Spherical particle sampling
Stochastic media

ABSTRACT

Chord length sampling method in Monte Carlo simulations is a method used to model spherical particles with random sampling technique in a stochastic media. It has received attention due to the high calculation efficiency as well as user convenience; however, a technical issue regarding boundary effect has been noted. In this study, after analyzing the distribution characteristics of spherical particles using an explicit method, an alternative chord length sampling method is proposed. In addition, for modeling in finite media, a correction method of the boundary effect is proposed. Using the proposed method, sample probability distributions and relative errors were estimated and compared with those calculated by the explicit method. The results show that the reconstruction ability and modeling accuracy of the particle probability distribution with the proposed method were considerably high. Also, from the local packing fraction results, the proposed method can successfully solve the boundary effect problem. It is expected that the proposed method can contribute to the increasing of the modeling accuracy in stochastic media.

1. Introduction

Stochastic media with randomly distributed spherical particles have been utilized for very high temperature reactors (pebble bed and prismatic reactors), radiation shielding materials, and the blankets of fusion reactors. For spherical particle modeling in Monte Carlo (MC) simulations, three kinds of methods are known: repeated structure, explicit method, and chord length sampling (CLS) method. The CLS is a modeling method that randomly samples the chord lengths on the ongoing neutron track during the MC simulation. The CLS method has high calculation efficiency because the MC simulation can be pursued with few geometries as well as automatic modeling of stochastic geometries. The CLS method was first proposed by Zimmerman and Adams [1]. After that, Murata et al [2] and Donovan et al [3] proposed the

* *Corresponding author.*
E-mail address: jkkim1@hanyang.ac.kr (J.K. Kim).

http://dx.doi.org/10.1016/j.net.2015.03.005
1738-5733/Copyright © 2015, Published by Elsevier Korea LLC on behalf of Korean Nuclear Society.

sampling scheme for the calculation of multiplication factors. Recently, many works have attempted to increase or to confirm the accuracy of CLS [4–6]. A technical issue referred to as the *boundary effect* has been noted when trying to confirm the accuracy of the CLS method [7]. In finite stochastic media, spherical particles cannot be located outside of the medium boundaries; therefore, the volume packing fraction is gradually decreased at the region near the boundary of the stochastic media. Also, the number density in the center region (which is not affected by the wall boundaries) is changed. Fig. 1 is an example of the failure in treating the boundary effect using CLS in a previous study [7]. With resampling scheme in the CLS method, only the track lengths are simulated in the Monte Carlo simulation. Therefore, the spherical particle resampling with the method developed in the previous study was pursued near the boundary as the positions of the spherical particle cannot be properly considered.

In this study, an alternative CLS method based on the geometrical cross section of spheres was proposed to increase the sampling accuracy in finite stochastic media. First, the characteristics of stochastic particle distribution were analyzed, and then corrections were applied to the proposed method. Finally, the proposed method was verified.

2. Methods

The alternative CLS method proposed in this study is a sampling method of the center position for the spherical particle geometry modeling. The conventional CLS method samples the chord length from the current position to the surface of the sphere (Fig. 2A). As shown in Fig. 2B, the proposed method samples the center position of the sampled particle. Hence, it gives an advantage in treating the boundary effect of finite stochastic media because the sphere's location is known.

To develop the proposed sampling method with high accuracy, analysis of the center position distribution of the spherical particles is essential when sampling the spherical particle. In the next section, the distribution properties of the center positions in stochastic media were analyzed with the explicit method. Using the information from the following section, geometry sampling and modeling methods were proposed.

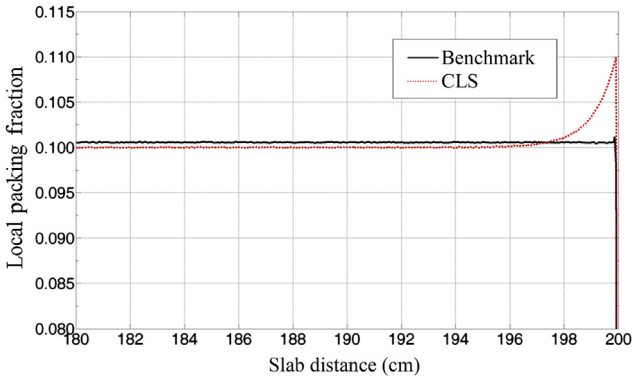

Fig. 1 – Spatial distribution of local packing fractions estimated in a previous study [7]. Source: http://www.tandfonline.com/doi/full/10.1080/00411450.2011.639432, copyright holder: Taylor & Francis Group, LLC, year of copyright: 2011.

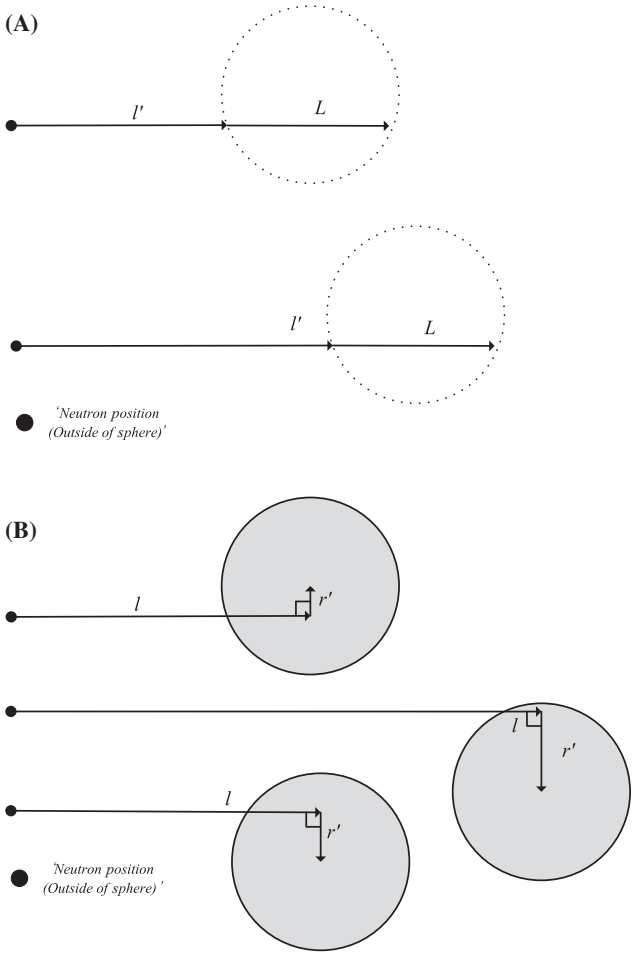

Fig. 2 – Introduction of schemes with the conventional chord length sampling (CLS) and proposed methods. (A) Sampling of chord lengths with conventional CLS method. (B) Sampling of particle position in the proposed method.

2.1. *Analysis of the random spherical particle distribution*

For the analysis of the distribution of the spherical particles, a benchmark problem was set. The medium is a 102 cm × 22 cm × 22 cm hexahedron, and the radius (r) of the spherical particles, which is filled in the medium, is 1 cm. For the 10%, 20%, 30%, and 40% volume packing fractions, the particle positions were randomly sampled with the modified random sequential addition method [8]. In the modified random sequential addition method, the particles are first sampled in the medium without considering the overlaps of the spherical particles. Then, the particles, which are overlapped with each other, are moved with $0.1r$ length as shown in Fig. 3. If the particles are moved to the out-of-boundary of the medium, they are removed and re-sampled in the medium. The movement process is repeated and stopped until

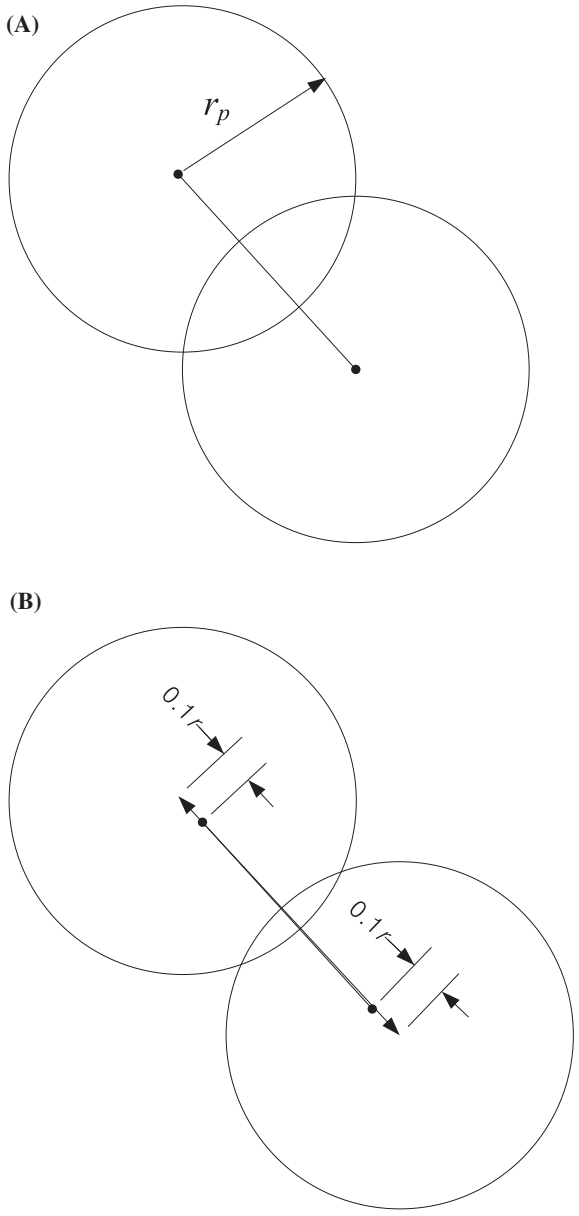

Fig. 3 – Movement scheme for the overlapped spheres with the modified random sequential addition method. (A) Before movement. (B) After movement.

the particles are located without any overlap. For each packing fraction, 100 benchmark problems were generated. The modeling results are shown in Fig. 4. To analyze the distribution properties, a center region was defined with a size of 100 cm × 20 cm × 20 cm, as shown in Fig. 5. A starting position outside the spheres is randomly selected on the left surface of the center region. The track lengths passing though the spherical particles on the vertical direction of the front surface are estimated from the starting position to the right surface of the center region. The volume packing fraction is defined as a fraction of the particle volume in the unit medium volume. Therefore, the volume packing fractions employing the track length estimation method can be estimated by Eq. (1).

$$PF = \sum_j \frac{\sum_i L_{i,j}}{D_j} \tag{1}$$

where PF is the volume packing fraction of the spherical particles, $L_{i,j}$ is a track length passing through i^{th} spherical particle at j trial number, and D_j is the distance from the left surface to right surface of the center region at each trial number. Using Eq. (1), the packing fractions in the center region were calculated as given in Table 1. Also, the probability density distributions of the l and r' lengths, which are the parallel and vertical lengths from the neutron to the particle, as shown in Fig. 2B, were evaluated.

The results of the length distributions are shown in Figs. 6 and 7. The results show two distribution properties. First, the l length sampling probability follows an exponential distribution at $l > r_p$, and the sampling probability at $l < r_p$ is gradually decreased as the sampled position approached the starting position. Second, as shown in Fig. 7, <L>, which is the average chord length passing through the spherical particle, is not a constant at $l < r_p$. Based on the information of the particle distribution properties, the alternative CLS method was proposed.

2.2. *Proposal of a spherical particle sampling method*

In this study, the alternative CLS method and strategy were proposed from a method used for Dancoff factor analysis [9]. First, the spherical particles are assumed to be huge nuclides, as shown in Fig. 8. Then, the particles have a geometrical microscopic cross section and number density as given in the following equations:

$$\sigma_p = \pi \cdot r_p^2 \tag{2a}$$

$$\overline{\rho} = \frac{n_t}{V_{med}} \tag{2b}$$

where r_p is the radius of the sphere, σ_p is the geometrical microscopic cross section of the spheres, n_t is the number of the spheres in the medium, and V_{med} is the volume of the medium excepting the total volume of spherical particles. Hence, the geometrical macroscopic cross section, Σ, is given by Eq. (3).

$$\Sigma = \overline{\rho} \cdot \sigma_p \tag{3}$$

For spherical particle sampling in 3D medium, the parallel and vertical locations of the sphere on the neutron ongoing track should be sampled as shown in Fig. 9. The probability density function for the parallel length (l) sampling on the neutron ongoing direction is assumed to be the probability density function based on nuclide reaction. Also, the vertical length (r') and azimuthal angle (θ) are uniformly sampled over the microscopic cross section area for the decision of sampled sphere position in 3D space. The probability density functions for the cylindrical coordinate system are given as follows:

$$p(l) = \sum e^{-\Sigma l} \quad [0 < l < \infty] \tag{4}$$

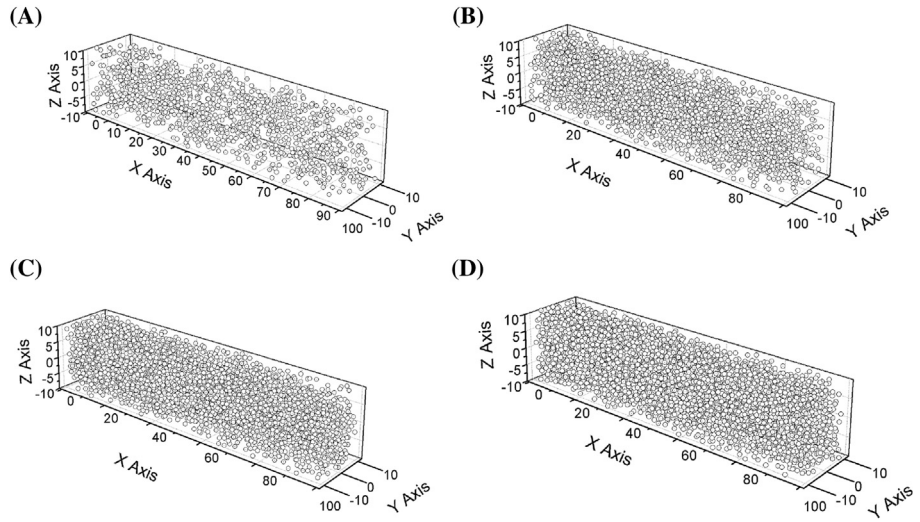

Fig. 4 – Modeling result of randomly packed spheres using the modified random sequential addition method [8]. (A) 10% packing fraction; (B) 20% packing fraction; (C) 30% packing fraction; and (D) 40% packing fraction. Source: Conference proceeding of "Korea Nuclear Society(KNS) meeting".

$$p(r') = \frac{2}{r_p^2} r' \quad [0 < r' < r_p] \tag{5}$$

$$p(\theta) = \frac{1}{2\pi} \quad [0 < \theta < 2\pi] \tag{6}$$

However, as described in *Analysis of the random spherical particle distribution* section, the exponential distribution in Eq. (4) cannot represent realistic particle distribution of the spherical centers because the initial location for the spherical particle sampling is always located outside of the spheres. To consider the probability distribution in *Analysis of the random spherical particle distribution* section, we propose a rejection technique in which rejection and resampling are pursued when a sampled particle overlaps with the neutron position. To calculate the rejection probability, we start with the definition of the sampling probability of a spherical particle at location l. s is defined as the distance between the neutron position and a sampled spherical particle position. As shown in Fig. 10A, s can be simply calculated with Eq. (7).

$$s = \sqrt{r'^2 + l^2} \tag{7}$$

If s is smaller than r_p ($s < r_p$), the sampled particle is overlapped with the neutron position as shown in Fig. 10A. Also, if $s \geq r_p$, the spherical particle can be sampled for $r' \geq \sqrt{r_p^2 - l^2}$ as shown in Fig. 10B. Therefore, with the rejection technique, the conditional particle sampling probability with the sampled length l can be expressed with r' sampling probability as the following equation:

$$p_s(ps|l) = \left\{ \begin{array}{l} p_s(ps|l \geq r_p) = \int_0^{r_p} \frac{2}{r_p^2} r' dr' = 1 \\ p_s(ps|l < r_p) = \int_{\sqrt{r_p^2 - l^2}}^{r_p} \frac{2}{r_p^2} r' dr' = \frac{l^2}{r_p^2} \end{array} \right\} \tag{8}$$

where $p_s(ps|l \geq r_p)$ is the particle sampling probability (ps) without rejection at given length l for $l \geq r_p$ and $p_s(ps|l < r_p)$ is the particle sampling probability without rejection at given length l for $l < r_p$. Eq. (8) means that sampled particles with $l \geq r_p$ are not rejected, while sampled particles with $l < r_p$ are rejected at a decreasing rate as l increases. Using Eqs. (4) and (8), the l length sampling probability with the rejection technique can be derived as in Eq. (9).

$$p_{sampled}(l) = p(l) p_s(ps|l) = H(l) H(r_p - l) \frac{l^2}{r_p^2} \sum e^{-\Sigma l} + H(l - r_p) \sum e^{-\Sigma l} \tag{9}$$

where H is the Heaviside function to express the discrete condition in Eq. (8). However, Eq. (9) cannot be directly used for

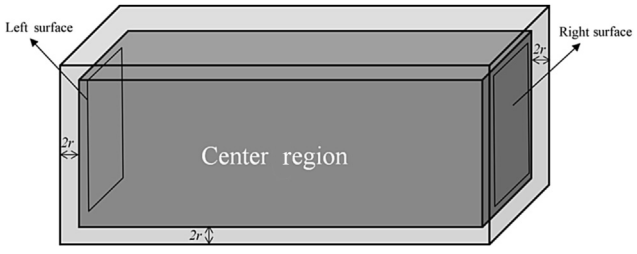

Fig. 5 – Center region in the hexahedron medium.

Table 1 – Volume packing fractions in the center region with the modified random sequential addition method [8].

Average volume packing fraction	Volume packing fraction in the center region	σ
0.1	0.12515	±0.00035
0.2	0.25181	±0.00062
0.3	0.37389	±0.00047
0.4	0.49834	±0.0006

Source: Conference proceeding of "Korea Nuclear Society(KNS) meeting".

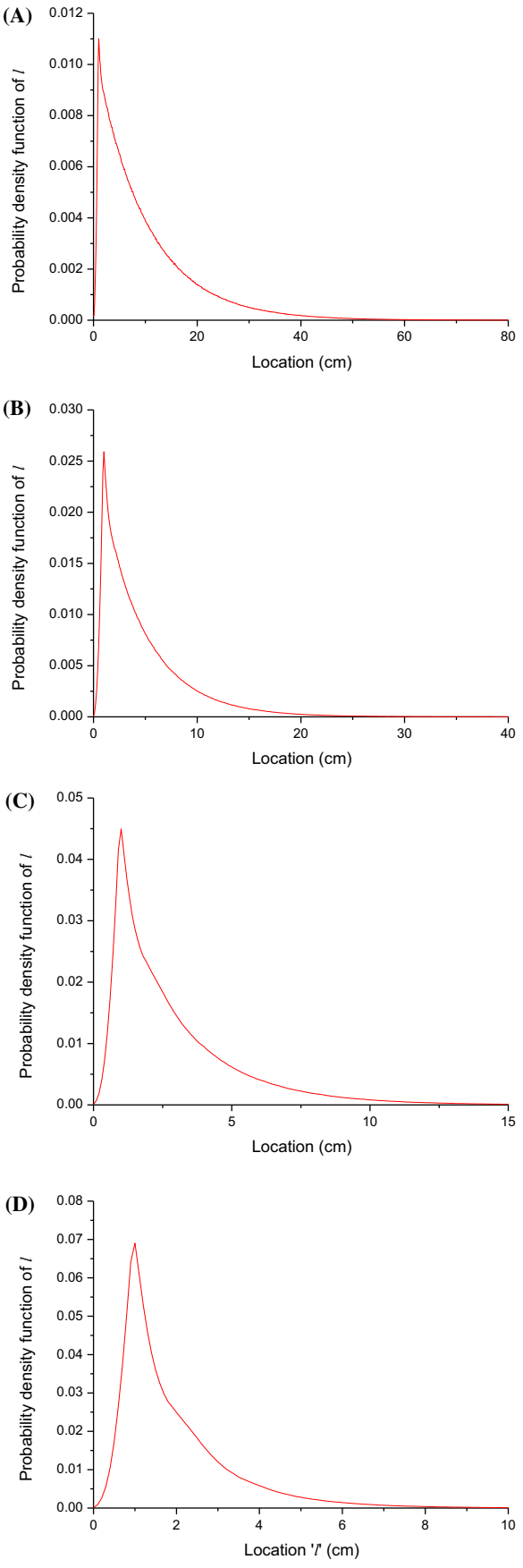

Fig. 6 – Probability density distributions of l at different lengths with explicit method. (A) 0.12515 packing fraction; (B) 0.25181 packing fraction; (C) 0.37389 packing fraction; and (D) 0.49834 packing fraction.

the l length sampling because the total sampling probability is reduced ($p < 1$) by using our rejection technique. Hence, to compensate for the reduced probability, Σ^* is defined as the corrected macroscopic cross section. In using Σ^*, the initial volume packing fraction must be conserved. Thus, to calculate Σ^*, the average volume packing fraction is defined by the average track length (or chord length) in Fig. 11 as follows:

$$PF = \frac{\overline{l_p}}{\overline{l_t}} \tag{10}$$

where PF is the average volume packing fraction, $\overline{l_p}$ is the average track length passing through the spherical particle, and $\overline{l_t}$ is an average of the total track length. As shown in Fig. 11, the total track length (l_t) and the track length passing sphere (l_p) are related with the l and r' by the following equations:

$$l_t = l + \frac{l_p}{2} \tag{11}$$

$$l_p = 2\sqrt{r_p^2 - r'2} \tag{12}$$

Using Eqs. (4), (5), (11) and (12) with the rejection boundary used in Eq. (8), the average track lengths can be calculated from Eqs. (13) and (14).

$$\overline{l_t} = \int_0^{r_p} dl \int_{\sqrt{r_p^2 - l^2}}^{r} dr' \frac{2r'}{r_p^2} \Sigma^* e^{-\Sigma^* l} \left(l + \sqrt{r_p^2 - r'^2} \right) + \int_{r_p}^{\infty} dl \int_0^{r_p} dr' \frac{2r'}{r_p^2} \Sigma^* e^{-\Sigma^* l} \left(l + \sqrt{r_p^2 - r'^2} \right) \tag{13}$$

$$\overline{l_p} = \int_0^{r_p} dl \int_{\sqrt{r_p^2 - l^2}}^{r} dr' \frac{2r'}{r_p^2} \Sigma^* e^{-\Sigma^* l} \left(2 + \sqrt{r_p^2 - r'^2} \right) + \int_{r_p}^{\infty} dl \int_0^{r_p} dr' \frac{2r'}{r_p^2} \Sigma^* e^{-\Sigma^* l} \left(2 + \sqrt{r_p^2 - r'^2} \right) \tag{14}$$

Substituting Eqs. (13) and (14) to Eq. (10), Eq. (15) is then derived as follows:

$$A\left(\Sigma^*\right)^2 + Br_p\Sigma^* + B = Be^{\Sigma^* r_p} \tag{15}$$

where $A = 2r_p^2(1 - PF)$ and $B = (4 - 5\ PF)$.

Eq. (15) cannot be directly solved, and thus, numerical methods are recommended. Using the Σ^* estimated from Eq. (15), the spherical particle modeling with the rejection technique proposed in this study is performed by the algorithm described in Fig. 12 with the following procedure:

Step 1: l is sampled with Eq. (16) with a random number ξ

$$l = -\frac{\ln(\xi)}{\Sigma^*} \tag{16}$$

Step 2: r' is sampled with Eq. (17) with a random number ξ

$$r' = r_p\sqrt{\xi} \tag{17}$$

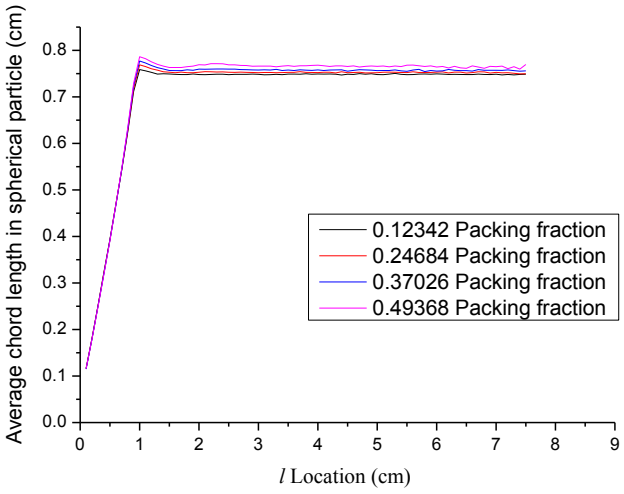

Fig. 7 – Average chord length < l > passing through spheres at location l.

Step 3: if s ($=\sqrt{l^2+r'^2}$) is $< r_p$, go to Step 1 (overlapped case with neutron position); otherwise, go to Step 4.

Step 4: Considering the neutron position and ongoing direction, new sphere positions are sampled with Eqs. (18) or (19).

- For $1-\frac{2}{w0} > 0.1$;

$$x_{sp} = x_n + lu_0 + r'\frac{(\xi_1 u_0 w_0 - \xi_2 v_0)}{\sqrt{\xi_1^2+\xi_2^2}(1-w_0^2)} \tag{18a}$$

$$y_{sp} = y_n + lv_0 + r'\frac{(\xi_1 v_0 w_0 - \xi_2 u_0)}{\sqrt{\xi_1^2+\xi_2^2}(1-w_0^2)} \tag{18b}$$

$$z_{sp} = z_n + lw_0 - r'\frac{\xi_1\sqrt{(1-w_0^2)}}{\sqrt{\xi_1^2+\xi_2^2}} \tag{18c}$$

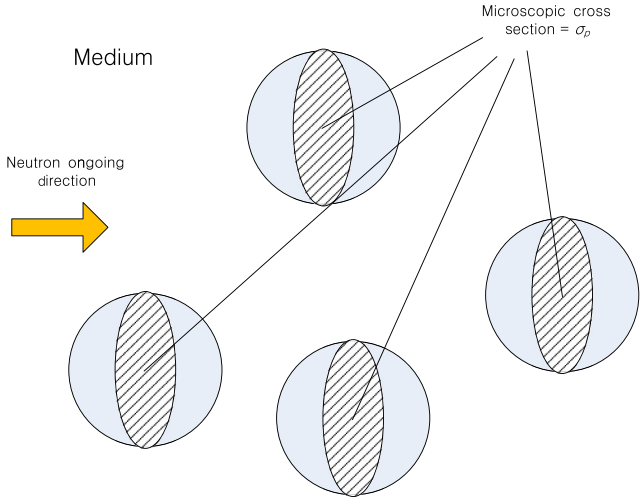

Fig. 8 – Basic principle of the proposed modeling method.

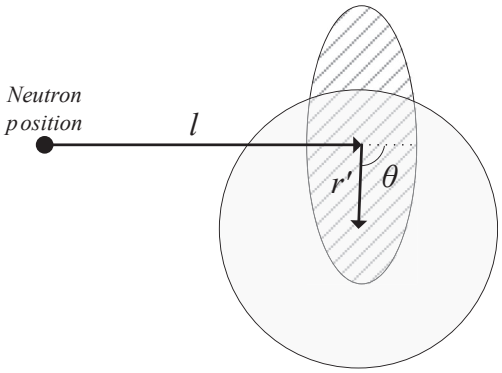

Fig. 9 – Sampling scheme with the proposed method.

- Otherwise;

$$x_{sp} = x_n + lu_0 + r'\frac{(\xi_1 u_0 v_0 - \xi_2 w_0)}{\sqrt{\xi_1^2+\xi_2^2}(1-v_0^2)} \tag{19a}$$

$$y_{sp} = y_n + lv_0 + r'\frac{\xi_1\sqrt{1-v_0^2}}{\xi_1^2+\xi_2^2} \tag{19b}$$

$$z_{sp} = z_n + lw_0 + r'\frac{(\xi_1 w_0 v_0 - \xi_2 u_0)}{\sqrt{\xi_1^2+\xi_2^2}(1-v_0^2)} \tag{19c}$$

where (x_{sp}, y_{sp}, z_{sp}) are the new sphere positions sampled, (x_n, y_n, z_n) are the neutron positions, (u_0, v_0, w_0) are the unit vectors of the neutron ongoing direction, and ξ_1 and ξ_2 are random numbers. Using the rejection method in Step 3, the sampling probability is naturally reduced near the neutron position as described in *Analysis of the random spherical particle distribution* section.

Step 5: If the sampled spherical particle overlaps with the boundary of the stochastic medium or is outside the stochastic medium, it is rejected; otherwise, the particle sample is accepted and the sphere sampling is stopped.

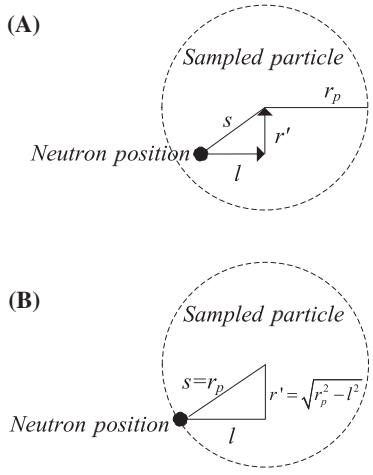

Fig. 10 – Overview of spherical particle sampling and rejection. (A) Overlapped case (rejected) and (B) boundary condition for using the rejection technique.

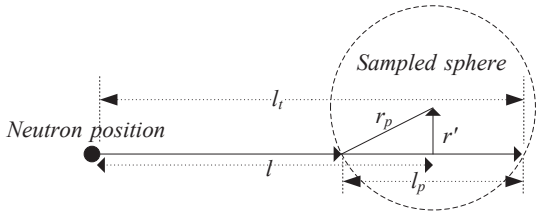

Fig. 11 – Estimation of track lengths for the calculation of σ^* with sampled sphere.

Step 6: If the rejection is used in Step 5, the other spherical particles, which are located behind the rejected spherical particle, cannot be sampled as shown in Fig. 13; thus, a temporal neutron position is decided at the surface of the rejected particle as shown in Fig. 13. If the temporal neutron position is outside of the stochastic boundary, the particle sampling procedure is stopped; otherwise, go to Step 1 with the temporal neutron position.

2.3. *Proposal of number density correction method*

Using the proposed method, modeling of spheres in infinite stochastic media can be effectively and accurately pursued. However, for finite media, the boundary effect should be properly accounted. Using the proposed method in Step 5, the sampling frequency near the wall boundary is naturally reduced by the rejection method. Thus, the average number density of the spherical particles is also reduced. In this study, a correction method to compensate for the average number density or packing fraction is proposed. As shown in Fig. 14A, the sampled spherical particle cannot be located in *Region B* or *Out-of-Boundary*. Thus, the number density is continually decreasing as the boundary of the medium is approached using the rejection method in Step 5. To describe this phenomenon, first, an intersection volume (between *Region A* and the spherical particle) is defined as a region that the spherical particles can be located. Then, the particle number density, $\rho(\underline{r})$, near the medium boundary at location $\underline{r}$ (a temporal position in a stochastic medium) is proportionally decreased by the volume fraction, which is the intersection volume per total volume of the spherical particle.

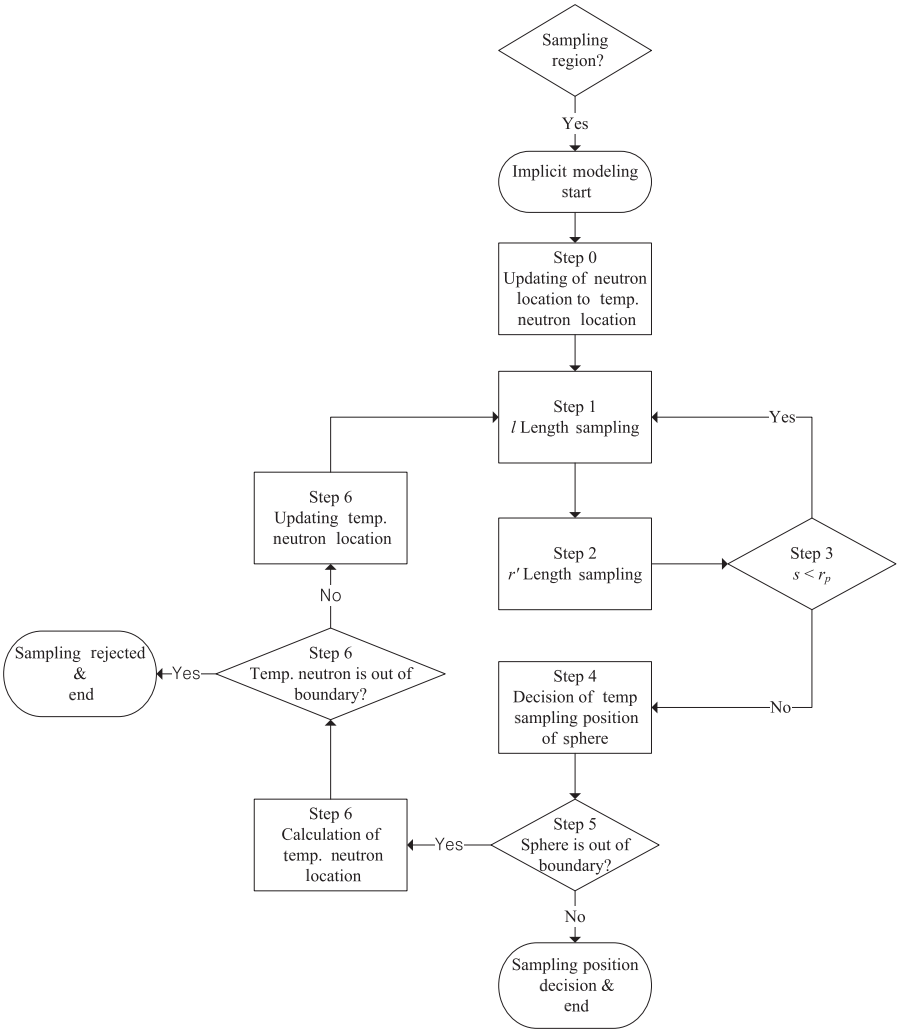

Fig. 12 – Overall algorithm of the proposed modeling method.

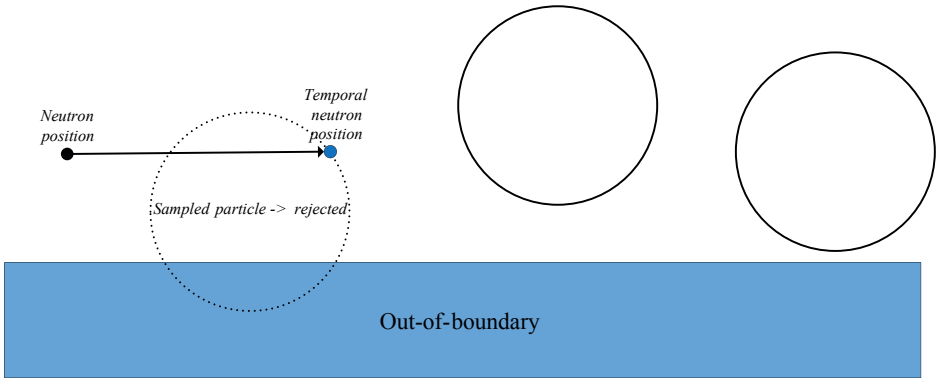

Fig. 13 – Step 5 rejection method with a stochastic medium boundary.

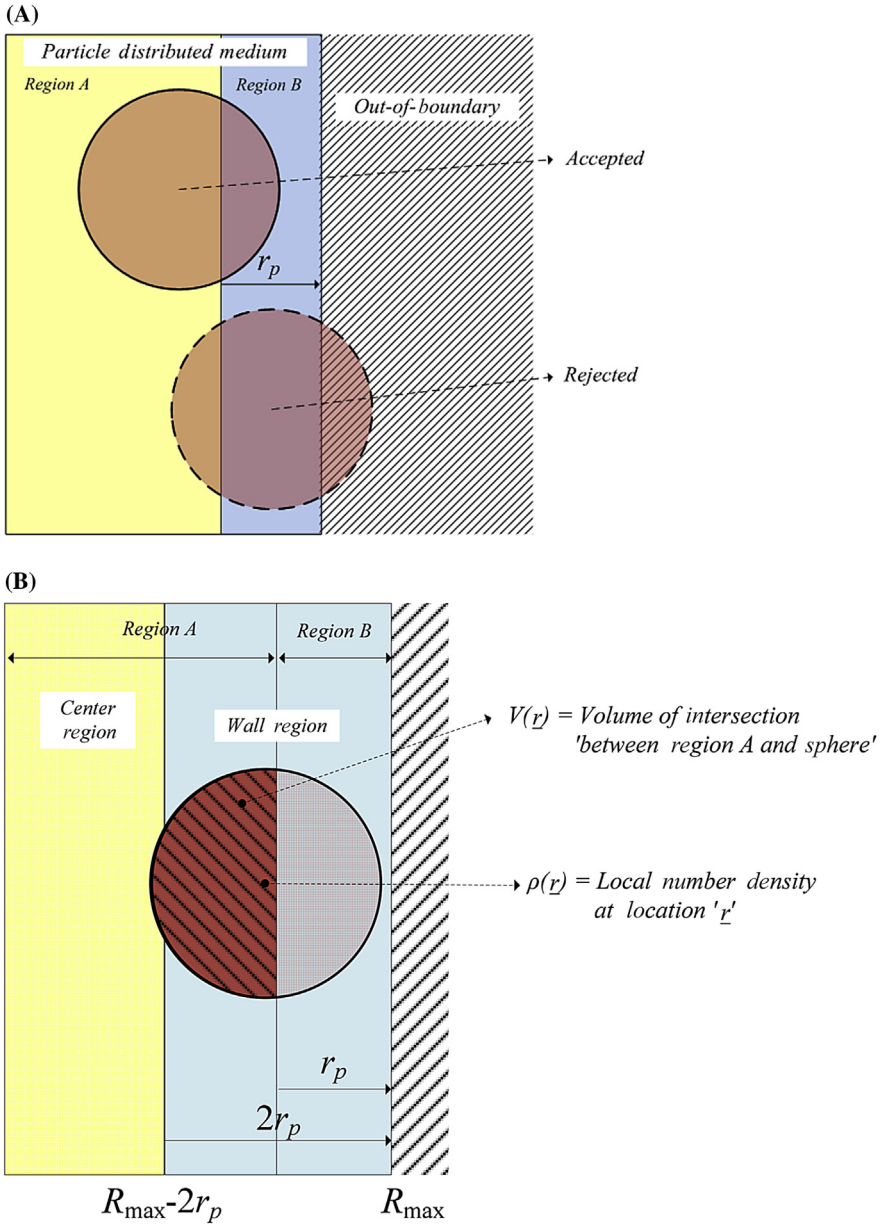

Fig. 14 – Overview of the local number density calculation. (A) Sampling and rejection regions in the particle distributed medium and (B) calculation of local number density.

The wall region is defined as the region in which the number density is changed by the wall effect, as shown in Fig. 14B. The number density in the center region of Fig. 14B is constant because there is no wall effect. The local number density is calculated using Eq. (20).

$$\begin{cases} \rho(\underline{r}) = \dfrac{V(\underline{r})}{V_T}\rho_c, & \text{if } \underline{r} \text{ is in Wall Region} \\ \rho(\underline{r}) = \rho_c, & \text{otherwise} \end{cases} \tag{20}$$

where $V(\underline{r})$ is the intersection volume between Region A and the sphere in Fig. 13, V_T is the volume of the spherical particle, and ρ_c is the number density in the center region. The number of the particles in the regions is conserved; hence, ρ_c can be calculated using Eq. (23).

$$n_t = n_c + n_w \tag{21}$$

$$\overline{\rho}\cdot V_{med} = \rho_c \cdot V_c + \overline{\rho_w}\cdot V_w \tag{22}$$

$$\rho_c = \frac{\overline{\rho}\cdot V_{med} - \overline{\rho_w}\cdot V_w}{V_c} \tag{23}$$

where n_c is the number of particles in the center region, n_w is the number of the particles in the wall region, V_c is the volume of the center region, $\overline{\rho_w}$ is the average number density in the wall region, and V_m is the volume of the wall region.

In the proposed method with boundary effect correction, ρ_c is used instead of $\overline{\rho}$ in Eq. (3) for wall effect correction. Also, the modified volume packing fraction to use in Eq. (15) can be calculated from the following equation:

$$PF_c = \rho_c \cdot \frac{3}{4}\pi r_p^3 \tag{24}$$

In Eq. (23), the parameters can be easily obtained from the initial condition, except for the average number density in the wall region. We derived methods to calculate the average number density in the wall region for three representative boundary types: plane, sphere and cylinder.

(1) Plane boundary

The number density in the wall region is gradually decreased by the $V(\underline{r})/V_T$ volume fraction as given in Eq. (20). For the plane boundary, the intersection volume $V(\underline{r})=V(x)$ in the wall region is calculated from Eq. (25).

$$V(x) = \int_{-r_p}^{R_{max}-r_p-x} \pi\left(\sqrt{r_p^2 - x'^2}\right)^2 dx' \tag{25}$$

Fig. 15 shows the results of the relative number density calculated from Eqs. (20) and (25). The average number density in the wall region for the wall effect correction is estimated from the Eq. (26).

$$\overline{\rho_w} = \frac{\int_0^{2r_p} A\cdot\rho(r)dr}{\int_0^{2r_p} A dr} \tag{26}$$

where A is a constant for the unit area of the plane.

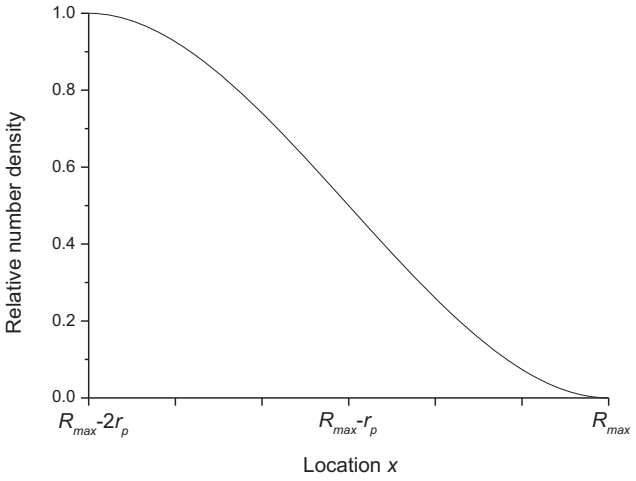

Fig. 15 – Distribution of the relative number density for the plane boundary.

(2) Sphere boundary

The intersection volume $V(\underline{r})=V(r)$ for the spherical medium can be divided as shown in Fig. 16. One is the partial volume of the sampled particle, and another is the partial volume of the spherical medium. Therefore, the intersection volume, $V(r)$, can be calculated from the sum of the two partial region volumes.

$$V(r) = V_{p1}(r) + V_{p2}(r) \tag{27}$$

where $V_{p1}(r)$ is the partial region volume of the spherical particle and $V_{p2}(r)$ is the partial region volume of the spherical medium. The partial volumes ($V_{p1}(r)$ and $V_{p2}(r)$) can be calculated from Eqs. (28) and (29), respectively.

$$V_{p1}(r) = \int_{r-p(r)}^{r_p} \pi\left(\sqrt{r_p^2 - r'^2}\right)^2 dr' \tag{28}$$

$$V_{p2}(r) = \int_{p(r)}^{R_{max}-r_p} \pi\left(\sqrt{(R_{max}-r_p)^2 - r'^2}\right)^2 dr' \tag{29}$$

where

$$p(r) = \frac{(R_{max}-r_p)^2 - r_p^2 + r^2}{2r}$$

Fig. 17 is the relative number density in the wall region of the spherical medium calculated. The average number density of the wall region is calculated from Eq. (30).

$$\overline{\rho_w} = \frac{\int_{R_{max}^{-2r_p}}^{R_{max}} \rho(r)\cdot 4\pi r^2 dr}{\int_{R_{max}^{-2r_p}}^{R_{max}} 4\pi r^2 dr} \tag{30}$$

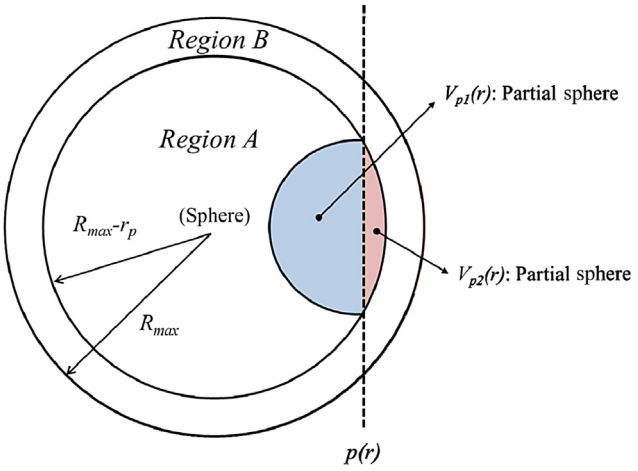

Fig. 16 – Partial division of the intersection volume for the spherical boundary.

(3) Cylinder boundary

It is impossible to derive directly the equation of the intersection volume $V(\underline{r})=V(r)$ for the cylinder boundary due to the generation of the integrated error function. For the calculation, a numerical approach is introduced. At first, the intersection region is divided into two radial subregions and axial subregions with unit length, Δz as shown in Fig. 18. Then, $V(r)$ is the sum of the divided cylinder volumes; hence, the equation is derived as Eq. (31).

$$V(r) = \sum_{i=1}^{n} \{V_{p3}(r, z_i) + V_{p4}(r, z_i)\} \tag{31}$$

where

$$\Delta z = r_p/n$$

$$z_i = \frac{2i-1}{2}\Delta z$$

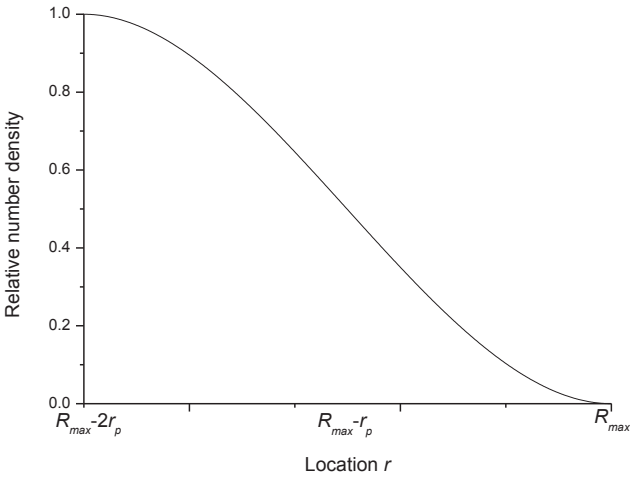

Fig. 17 – Distribution of the relative number density for the sphere boundary.

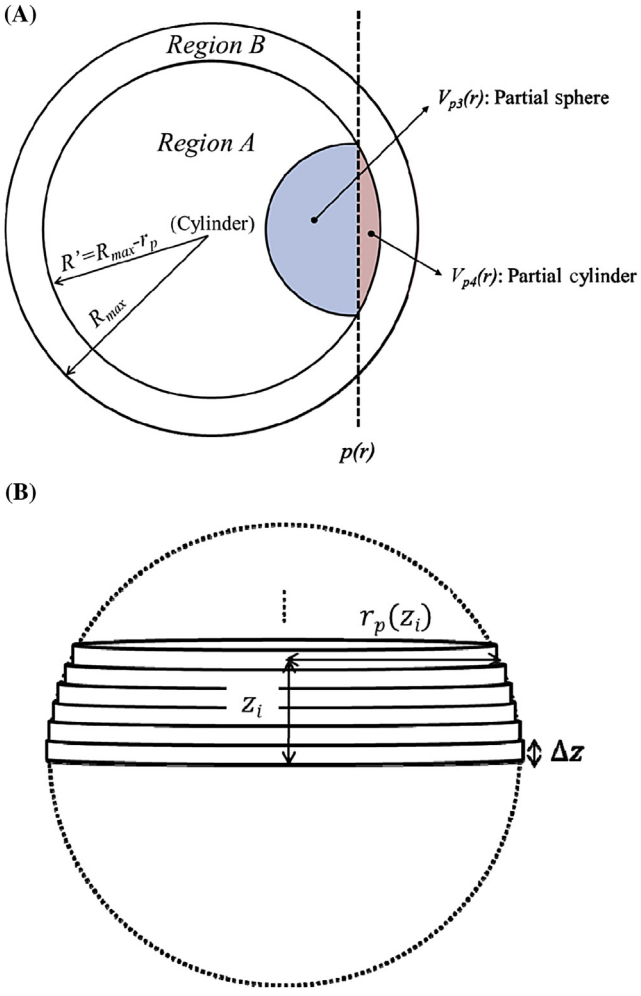

Fig. 18 – Partial division of the intersection volume for the cylindrical boundary. (A) Radial division of the intersection volume and (B) axial division of the intersection volume.

n = total number of axial divisions
$V_{p3}(r,z_i)$ = partial volume of the spherical particle at r and z_i
$V_{p4}(r,z_i)$ = partial volume of the cylindrical boundary at r and z_i

Each divided region is assumed to have a cylindrical shape as shown in Fig. 18B. As a result, the volume at each divided region can be calculated from Eqs. (32)–(35):

if $R_{max} - 2r_p(z_i) < r < R_{max}$;

$$V_{p3}(r, z_i) \approx \Delta z \left[\sum_{i=1}^{n} \frac{\pi}{2} r_p(z_i)^2 - \{r - p(r, z_i)\} \sqrt{r_p(z_i)^2 - \{r - p(r, z)\}^2} - r_p(z_i)^2 \arcsin\left[\frac{\{r - p(r, z)\}}{r_p(z_i)}\right] \right] \tag{32}$$

$$V_{p4}(r, z_i) \approx \Delta z \left[\sum_{i=1}^{n} \frac{\pi}{2} R'^2 - p(r, z_i) \sqrt{R'^2 - p(r, z_i)^2} - R'^2 \arcsin\left[\frac{p(r, z_i)}{R'}\right] \right] \tag{33}$$

and if $r < R_{max} - 2r_p(z_i)$;

$$V_{p3}(r, z_i) + V_{p4}(r, z_i) = r_p(z_i)^2 \Delta z \quad (34)$$

otherwise;

$$V_{p3}(r, z_i) + V_{p4}(r, z_i) = 0 \quad (35)$$

where $r_p(z_i)$ = radius of the divided spherical sub-region at $z_i = \sqrt{r_p^2 - z_i^2}$

$$R' = R_{max} - r_p$$

$$p(r, z_i) = \frac{R'^2 - R_p(z_i)^2 + r^2}{2r}$$

The relative number density using Eqs. (20) and (31) was calculated and the result is shown in Fig. 19. The average number density of the wall region is calculated from Eq. (36).

$$\overline{\rho_w} = \frac{\int_{R_{max}-2r_p}^{R_{max}} \rho(r) \cdot 2\pi r \cdot h dr}{\int_{R_{max}-2r_p}^{R_{max}} 2\pi r \cdot h dr} \cdot \frac{\sum_j^m \sum_i^n \rho(r_j, z_i) \cdot (r_j)}{\sum_j^m (r_j)} \quad (36)$$

where h is the unit height of the cylinder (constant) and

$$r_j = R_{max} - 2r_p + 2r_p \frac{j}{m}$$

3. Evaluation and validation

For the verification of the proposed method, three aspects were evaluated in this study. First, the sampled probability distributions for the benchmark problem in *Analysis of the random spherical particle distribution* section were estimated. Second, the local packing fractions in finite medium were evaluated. Finally, relative errors of the packing fractions for benchmark problems were evaluated and the results compared with those from the explicit method.

For the same conditions in *Analysis of the random spherical particle distribution* section, the spherical particle sampling from the proposed method was performed and repeated 10^8 times for each packing fraction. The results were calculated and compared with the results in the *Analysis of the random spherical particle distribution* section as shown in Fig. 20. The sampled probabilities with the proposed method and the explicit method give good coincidences with each other at low packing fraction. However, as shown in Fig. 20C,D, the packing fractions near the peak probability region have some discrepancies. Analysis shows that the discrepancies are caused by the assumption on the uniform distribution of the spherical particles used in this study. Fig. 21 shows an example on the radial packing fraction of the spherical particles with high packing fraction [10]. While the spherical particle distribution used in this study assumed to be a uniform distribution in stochastic media, the particle distributions with the explicit modeling method or experimental case give large fluctuations in the stochastic medium as shown in Fig. 21. Therefore, the packing fractions (estimated by the proposed method) highlighted as A and C in Figs. 20D and 21 are highly estimated compared to those of explicit method while the packing fraction in the region highlighted as B in Figs. 20D and 21 is a low estimate. As a result, for high packing fractions, the simulation accuracy using the method proposed in this study is relatively lower than that of low packing fractions. This phenomenon was analyzed as one of the limitations using the sampling based geometry modeling method, and therefore further study into the particle distribution with high pack fractions should be pursued in order to increase the accuracy of the sampling based methods.

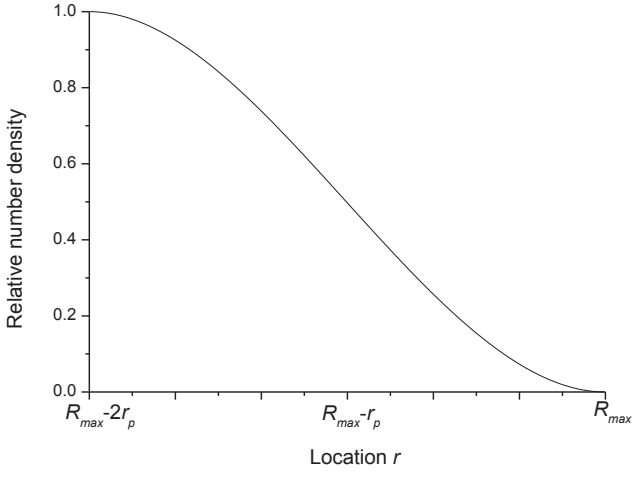

Fig. 19 – Distribution of the relative number density for the cylinder boundary.

To investigate the accuracy of the proposed method in the wall region (the boundary effect), a benchmark problem and results were introduced from a previous study [7]. The particle radius was set to 0.1 cm, and a 0.03 cm mesh was used for the record of the local packing fraction. Spherical particle sampling with a 0.1 cm radius was repeated 10^7 times in a 200 cm thick infinite plane. The local packing fraction was estimated by the track length estimator. Fig. 22 shows the results of the local packing fractions. The results near the wall region using the proposed method are in good agreement with the benchmark problem, while the local packing fraction near the wall boundary with the CLS method gives a larger relative error.

To confirm the accuracy of the proposed method in finite media, the particle sampling simulations for a fuel compact unit cell and a fuel pebble cell were pursued with benchmark problems. The cylindrical fuel zone in the fuel compact unit cell has radius 0.6225 cm and height 4.9276 cm. The TRISO particle in the fuel compact has radius 0.039 cm. For the pebble cell case, the spherical fuel zone has radius 2.5 cm, and the radius of the TRISO particle is 0.045 cm. The evaluations were performed in the PF range from 0.05 to 0.30 in 0.01 increments, and compared with those of the explicit method. Fig. 23A shows the results of the PF for the fuel compact unit cell, and Fig. 23B shows the results for the pebble unit cell. The relative errors of the results in both cases were within 0.5% of the proposed method.

4. Conclusion

This study proposes an alternative CLS method for spherical particle modeling in stochastic media. First, the

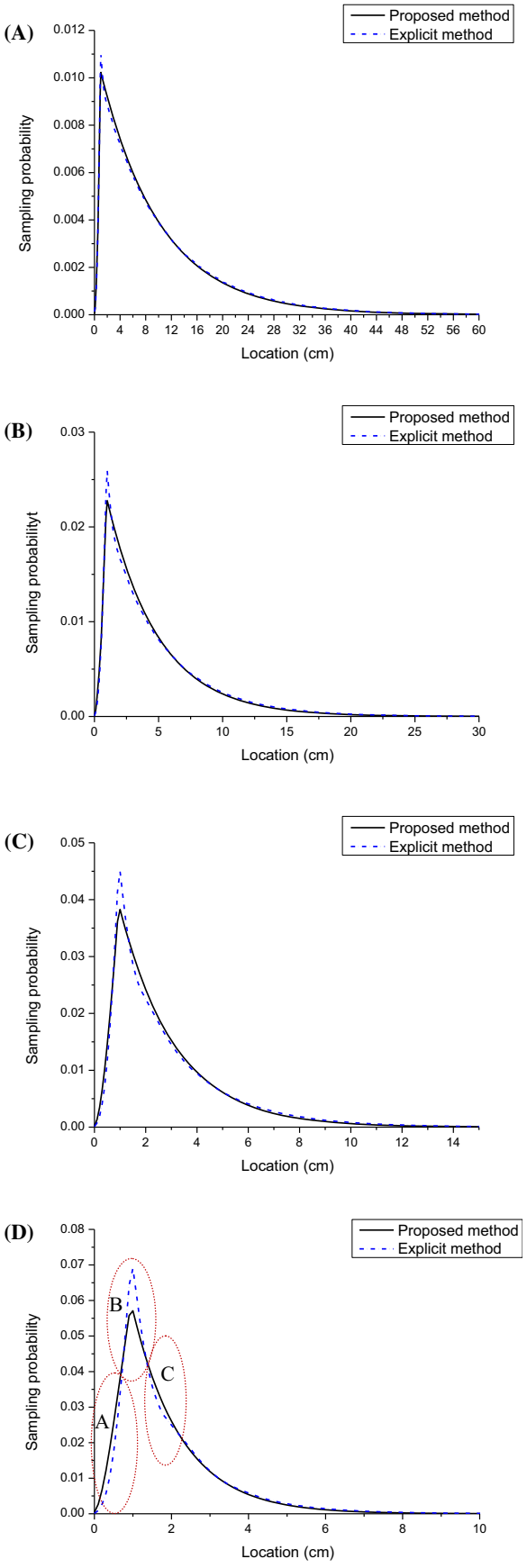

Fig. 20 – Probability density distributions at location *l* with the proposed method and the explicit method. (A) 0.12342 packing fraction; (B) 0.24684 packing fraction; (C) 0.37026 packing fraction; and (D) 0.49834 packing fraction.

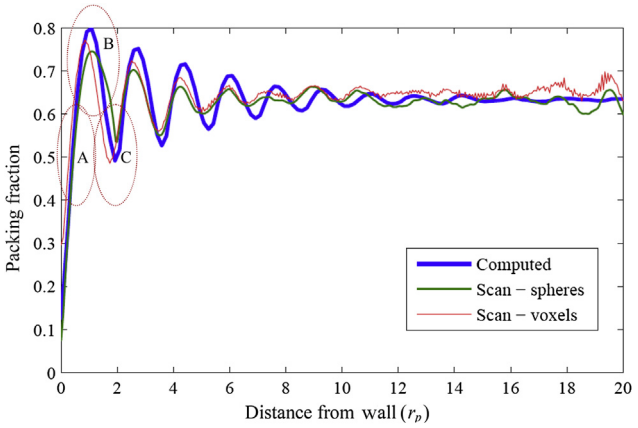

Fig. 21 – Profiles of radial packing fractions with computed pebble bed, voxels and sphere measurement data from tomography scan [10]. Source: Conference proceeding at PHYSOR, 2012.

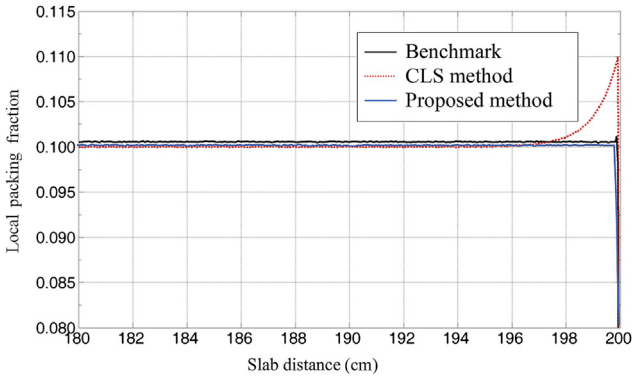

Fig. 22 – Distribution of local packing fraction with the proposed method and the other methods [7]. Source: http://www.tandfonline.com/doi/full/10.1080/00411450.2011.639432, copyright holder: Taylor & Francis Group, LLC, year of copyright: 2011.

characteristics of the particle center distributions in stochastic media were evaluated with explicit modeling, and then the distribution properties of the spherical particles were analyzed. To consider the properties, sampling and rejection methods were proposed with an analytical estimation method for the rejection probability. In addition, a correction method for the application in finite media was proposed. For verification, first, sampling probability distributions with the proposed method were evaluated and the results compared to those with explicit method. The analysis showed that the reproducibility of the probability distribution was confirmed. Second, the local packing fractions near the medium boundary were estimated and compared with the results of a previous study. We found that the proposed method can

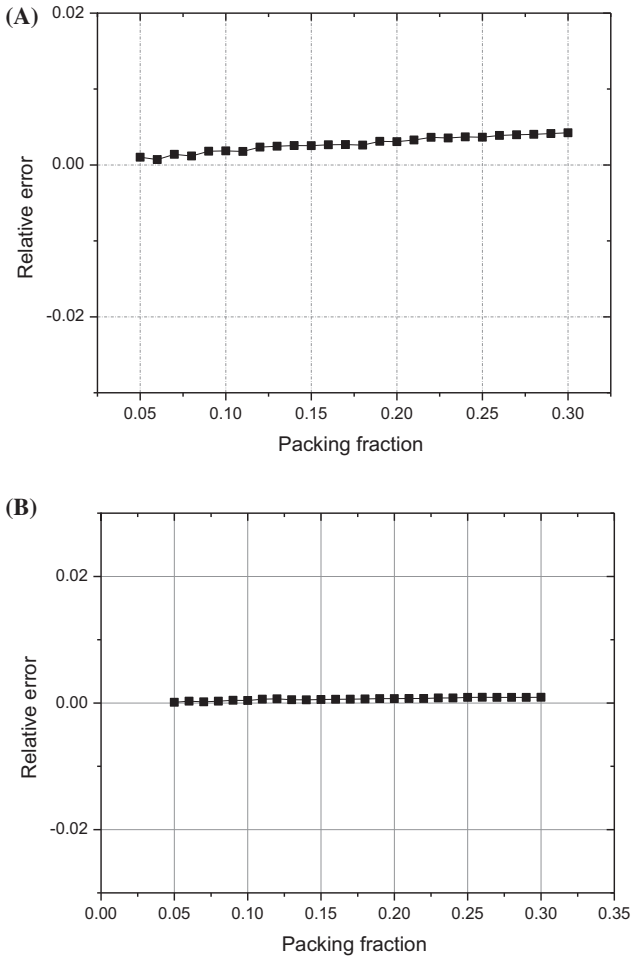

Fig. 23 – *Pf* relative errors between the proposed and explicit methods. (A) Cylindrical fuel compact and (B) spherical fuel pebble.

successfully reconstruct the local packing fraction near the boundary. Finally, the relative error of the average packing fractions was estimated and compared with the explicit methods. The results indicate that the proposed method has a good accuracy within 0.5% relative error. It is expected that the proposed method will contribute to increasing modeling accuracy and utilization of the CLS method in stochastic media.

5. Future work

A novel sampling-based modeling method of the spherical particles in stochastic media was proposed in this study. The proposed method uses different sampling distribution and procedure compared to the conventional CLS methods. Therefore, for the verification of the proposed method, the reactor characteristics of MC simulation such as the multiplication factor should be evaluated and compared with the other CLS methods. In this research, the basic distribution properties of the proposed method were only evaluated. For the future work, the reactor characteristics with a development of MC simulation code will be performed with the proposed method.

Conflicts of interest

All contributing authors declare no conflicts of interest.

Acknowledgments

This work was supported by the National Research Foundation of Korea (NRF) grant funded by the Korea government (MSIP; 2012M2A8A2025679), the Energy Efficiency & Resources of the Korea Institute of Energy Technology Evaluation and Planning (KETEP) grant funded by Korea government Ministry of Knowledge Economy (20121620100070), and the Innovative Technology Center for Radiation Safety (iTRS).

REFERENCES

[1] G.B. Zimmerman, M.L. Adams, Algorithms for Monte-Carlo particle transport in binary statistical mixture, Trans. American Nucl. Soc. 64 (1991) 287–288.
[2] I. Murata, A. Takahashi, T. Mori, M. Nakagawa, New sampling method in continuous energy Monte Carlo calculation for pebble bed reactors, J. Nuc. Sci. Technol. 34 (1997) 734–744.
[3] T.J. Donovan, T.M. Sutton, Y. Danon, Implementation of chord length sampling for transport through a binary stochastic mixture, in: Proceeding of Nuclear Mathematical and Computational Science: A Century in Review, Gatlinburg, Tennessee, 2003.
[4] D.R. Reinert, E.A. Schneider, S.R.F. Biegalski, Investigation of stochastic radiation transport methods in binary random heterogeneous mixtures, Nuc. Sci. Eng. 166 (2010) 167–174.
[5] C. Liang, W. Ji, F.B. Brown, Chord length sampling method for analyzing stochastic distribution of fuel particles in continuous energy simulations, Ann. Nucl. Energy 53 (2010) 140–146.
[6] C. Liang, W. Ji, A novel extension of chord length sampling method for TRISO-type fueled reactor applications, Ann. Nucl. Energy 71 (2014) 440–450.
[7] C. Liang, W. Ji, On the chord length sampling in 1-D binary stochastic media, Transport Theory Statistical Phys. 40 (2011) 282–303.
[8] J.Y. Lee, S.H. Kim, C.H. Shin, J.K. Kim, An analysis of spherical particles distribution randomly packed in a medium for the Monte Carlo implicit modeling, in: Transaction of the Korea Nuclear Society Spring Meeting, Jeju, Korea, 2014.
[9] S.H. Kim, et al., New strategy on the evaluation of Dancoff Factor in a pebble bed reactor using Monte Carlo method, Nucl. Technol. 177 (2012) 147–156.
[10] G.J. Auwerda, J.L. Kloosterman, D. Lathouwers, T.H.J.J. Van Der Hagen, Packing microstructure and local density variations of experimental and computational pebble beds, PHYSOR 2012 Advances in Reactor Physics Linking Research, Industry, and Education Knoxville, TN, USA, April 15–20, 2012.